ELSEVIER

Journal of Molecular Catalysis A: Chemical 104 (1996) 299–309

JOURNAL OF MOLECULAR CATALYSIS A: CHEMICAL

Redox and carbonylation chemistry of iridium species in the channels of H-ZSM-5 zeolite

T.V. Voskobojnikov [a], E.S. Shpiro [a], H. Landmesser [b], N.I. Jaeger [b], G. Schulz-Ekloff [b,*]

[a] *N.D. Zelinsky Institute of Organic Chemistry, Russian Academy of Sciences, 47, Leninsky Prospect, 117913 Moscow, Russia*

[b] *Institut fur Angewandte und Physikalische Chemie, Universität Bremen, 28334 Bremen, Germany*

Received 22 February 1995; revised 19 June 1995; accepted 13 July 1995

Abstract

Reduction of Ir/H-ZSM-5 by hydrogen yields Ir^0 clusters exhibiting a large positive XPS shift (1.4 eV) and an upward IR shift (25–30 cm^{-1}) of linearly bonded CO, both suggesting a strong electron deficiency. Ir clusters (< 1 nm) can be readily and rapidly reoxidised by the highly acidic hydroxyls (protons) with subsequent formation of $Ir^+(CO)_2$ gem-dicarbonyl even with residual CO. Reductive carbonylation of $Ir^+(CO)_2$ in the presence of larger amounts of CO and H_2O results in the formation of an iridium cluster carbonyl species, most likely tetra-Ir carbonyl, $Ir_4(CO)_{12}$ which is unstable and can be reversibly transformed into a precursor compound $Ir^+(CO)_2$. Displacement of NH_3 ligands originally coordinated to unreduced Ir^{3+} cations yields the formation of $Ir^{3+}(CO)_2$. This species undergoes stepwise reduction to $Ir^+(CO)_2$ and Ir^0–CO via the water–gas shift reaction.

1. Introduction

Iridium-containing zeolites were reported to be rather efficient catalysts for alkane conversion [1], nitric oxide reduction [2] and the carbonylation of methanol [3]. Other important aspects of Ir catalytic chemistry are related to the strong promoting effect provided by iridium in bimetallic Pt–Ir/Al_2O_3 catalysts for gasoline reforming [4]. The most extended studies on iridium dispersion and its catalytic reactivity including CO reactions have been performed with Ir/Al_2O_3 catalysts [5,6] and Ir-loaded zeolites (mainly faujasites) where the electronic state of iridium and its interaction with CO has been investigated [3,7–11]. One of the unique features of small iridium particles is their ability to form different carbonyl complexes which can be considered not only as a probe for the identification of different iridium oxidation states but also as the reactive intermediates in carbonylation reactions [3,10,12,13]. Quite recently [12–15] the 'ship-in-the-bottle' technique was applied to prepare different iridium carbonyls in NaY zeolite and on γ-Al_2O_3.

The dispersion of iridium metal particles and the reactivity toward CO in highly acidic zeolite matrixes, such as H-ZSM-5 is largely unknown. It is the aim of the present paper to identify oxidation states and dispersion of Ir clusters as well as Ir–CO species formed during CO adsorption on a mildly reduced Ir/H-ZSM-5 catalyst prepared by ion exchange. The methods of Fourier-transform infrared (FTIR) spectroscopy for the analysis of the probe CO, and of X-ray photoelectron

* Corresponding author. (+49-421)2182373/2250 Fax (+49-421)2184918, E-mail: jse@alf.zfn.uni-bremen.de

SSDI 1381-1169(95)00185-9

spectroscopy (XPS), for the detection of iridium oxidation states, are applied. Rapid reoxidation of small Ir^0 clusters by protons followed by the formation of $Ir^+(CO)_2$ under low CO pressure and its further carbonylation to $Ir_4(CO)_{12}$ under high CO pressure are documented.

2. Experimental

2.1. Materials

The Ir-loaded H-ZSM-5 (Ir/H-ZSM-5, $SiO_2/Al_2O_3=35$) sample was prepared by ion exchange of the H form of the parent zeolite with an aqueous solution of the $[Ir(NH_3)_5H_2O]^{3+}$ complex at 350 K. The complex was synthesized following the method reported by Palmaer [16]. Thereafter the specimen was washed in hot water and dried at ambient temperature. According to X-ray fluorescence analysis the content of iridium in the zeolite was 0.8 wt.%.

2.2. Techniques

XPS spectra were recorded with a Kratos XSAM 800 spectrometer with Al Kα radiation as X-ray source according to a procedure described earlier [17]. The C 1s line (BE 285.0 eV) from residual hydrocarbons and the Si 2p line (BE 103.5 eV) from the zeolite were used as the reference for charging correction. The sample was heated in argon flow up to 423 K, then reduced in streaming H_2 at the same temperature and cooled again in argon. The pretreatment was performed in the in situ reactor allowing the transfer of the sample into the spectrometer without any contact with air [17].

FTIR spectra of adsorbed CO were recorded with the Bio-Rad FTS 60A spectrometer operating with a resolution of 2 cm^{-1}. The material was pressed into thin wafers (4–6 mg cm^{-2}) inserted into a gold grid and positioned in the IR cell [8,18]. The prereduced sample was again treated with hydrogen in the FTIR cell at 423 K and $P_{H_2}=5\times10^3$ Pa for 30 min. Subsequently, hydrogen was pumped off (10^{-4} Pa) in a few minutes. All spectra of adsorbed CO were subjected to background subtraction of the spectra of identically treated samples but without CO. Carbon monoxide was also adsorbed onto H-ZSM-5 support containing no metals. These experiments were carried out under similar conditions as with Ir-loaded zeolite. Some harmonics were visible between 1800 cm^{-1} and 2030 cm^{-1}, however, due to very low intensity (by 10–50 times lower) they have no noticeable effect on the spectra of CO adsorbed on the iridium species. For clarity, the spectrum of the blank zeolite with CO is included in Fig. 2a.

To evaluate the influences of (i) CO partial pressure, (ii) time and (iii) temperature on formation and decomposition of IR carbonyl species, different kinds of treatments were performed, and the temporal changes of the species were followed.

(A) After removal of H_2 at 423 K, the specimen was cooled in vacuum to 300 K. 10–100 Pa CO was added for a certain interval, and then ca. 90% of the gas phase CO was pumped off. The spectra of the species formed in the different exposure times are recorded (Fig. 2).

(B) After removal of H_2, the specimen was kept in vacuum by continuous pumping for 3 h at 423 K. Then the sample was cooled to 300 K and CO was added at various pressures for 5 min in each case. Subsequently, the CO was pumped off continuously (10^{-4} Pa) and the spectra were recorded (Fig. 3).

(C) After removal of H_2 at 423 K, the specimen was heated to 523 K under 10^4 Pa CO for 3 h. Subsequently, CO was removed under continuous pumping.

For the study of the influence of temperature, spectra were taken (i) in the presence of CO at high pressure (8×10^3 Pa) in the IR cuvette, i.e., under static conditions (Fig. 4) and (ii) under continuous pumping, i.e., under dynamic conditions (Fig. 5). During the recording of the spectra the temperature program was interrupted, and the temperature was kept constant. A sample reduced in the IR cell at 623 K for 30 min and then evac-

Table 1
XPS analysis of Ir/H-ZSM-5

Sample	Ir/Si	Parameters of Ir $4f_{7/2}$ peak [a]	
initial	0.005	62.9 (75) [b]	64.0 (25)
reduced 423 K	0.003	62.0 (50)	63.4 (50)
$[Ir(NH_3)_5H_2O]Cl_3$		62.6 (100)	

[a] Obtained by peak synthesis.
[b] The values in the parentheses give the percentage of the Ir oxidation state.

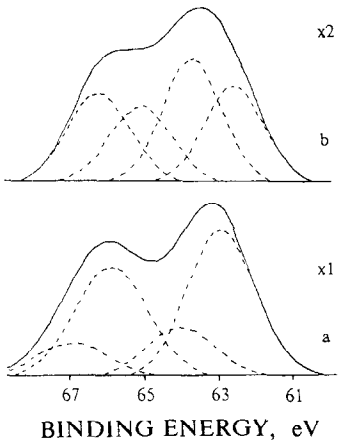

Fig. 1. XPS Ir 4f spectra of Ir/H-ZSM-5 (0.8 wt.% Ir): (a) as prepared; (b) reduced in H_2 at 423 K for 1 h. Dashed lines show the components obtained by peak synthesis.

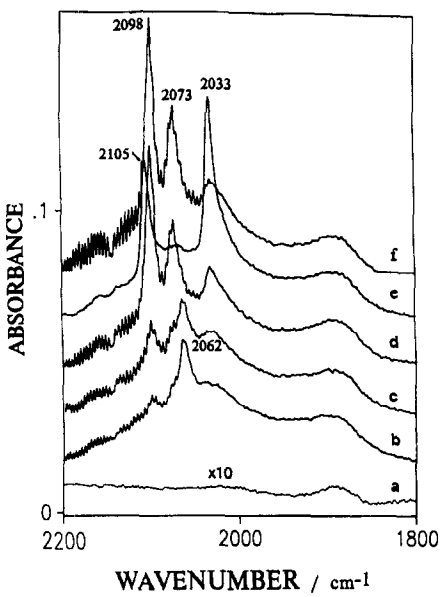

Fig. 2. IR spectra of Ir/H-ZSM-5 after CO exposure (10 Pa) at 300 K for different intervals and removal of 90% of the gas phase CO: (b) 1 s, (c) 1 min, (d) 10 min, (e) evacuation for 1 min, (f) 100 Pa CO for 1 min, spectrum (a) shows the bands of CO adsorbed on H-ZSM-5 support pretreated in a similar way.

uated for 1 h was used for background subtraction in the case of procedure (B). In the case of procedures (A) and (C) the spectra before reduction were used as background.

Electron micrographs were taken with Philips EM 420 electron microscope. Details of the technique were reported in [19]. No metallic particles were observed at a magnification of 5×10^5.

3. Results

3.1. X-ray photoelectron spectroscopy

XPS data are presented in Table 1 and in Fig. 1. Fig. 1a displays a XPS Ir 4f spectrum of the initial Ir/H-ZSM-5 sample. Peak synthesis procedure allowed to single out two Ir states: a major state (75%) with Ir $4f_{7/2}$ BE of 62.9 eV and a minor fraction with BE of 64.0 eV. The BE of 62.9 eV is rather close to the one observed for the Ir pentammine compound (Table 1).

The reduction of the ion-exchanged sample in hydrogen results in a significant change of the iridium oxidation state (Fig. 1b, Table 1). About 50% the of iridium atoms displays a spectrum with a lower BE of ca. 62 eV. The remainder of the iridium has a BE of 63.4 eV which is typical for Ir^{3+} cations. The Ir/Si surface atomic ratio decreases by 40% (Table 1) which can reflect either additional migration of metal cations into zeolite channels or the attenuation of the Ir signal caused by metal agglomeration. The first explanation is more probable since no metal particles were observed by TEM.

3.2. FTIR-spectroscopy

Fig. 2 depicts FTIR spectra obtained by treatment A. The spectrum 2a shows CO adsorption on H-ZSM-5 treated under the same conditions which is too weak to interfere with CO adsorbed on Ir. The spectrum of the Ir-loaded H-ZSM-5 (Fig. 2b) measured after exposure to 10 Pa CO for 1 second shows two distinct bands of CO stretchings at 2062 cm^{-1} and 1908 cm^{-1}. When

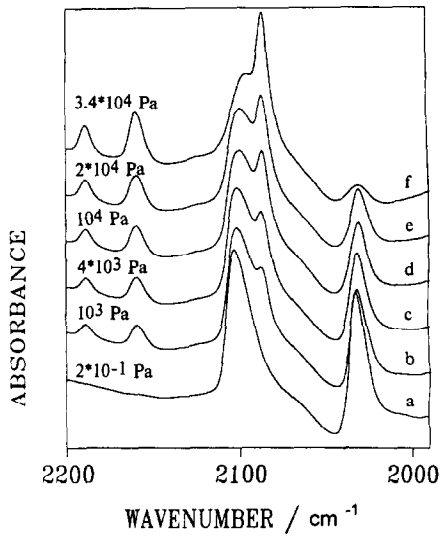

Fig. 3. IR spectra of Ir/H-ZSM-5 at 300 K after CO exposure at different pressures for 5 min and subsequent continuous pumping (10^{-4} Pa).

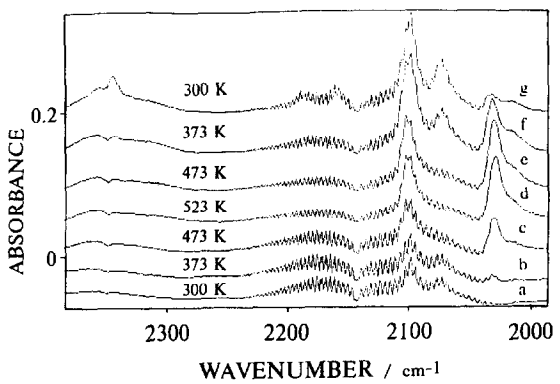

Fig. 4. The temperature dependence of IR spectra for Ir/H-ZSM-5 with CO at 8×10^{3} Pa, during heating from 300 K to 523 K (a–d) and during cooling from 473 K to 300 K (f–g).

CO is added for a prolonged time (spectra 2c and 2d) the band at 2062 cm^{-1} is replaced by three new bands at 2098, 2073 and 2032 cm^{-1}. The rotation modes of gaseous CO are also visible. Evacuation of CO removes the band at 2073 cm^{-1} and increases the bands at 2104 cm^{-1} and 2032 cm^{-1} (Fig. 2e). Readmission of CO at 100 Pa restored the original spectrum with bands at 2098 cm^{-1}, 2073 cm^{-1} and 2032 cm^{-1} (Fig. 2f). All spectra contain also a broad band located around 1900 cm^{-1}. Fig. 3 shows a set of spectra obtained for the specimen following treatment B. Spectrum 3a obtained after CO admission at 2×10^{-1} Pa shows two strong bands at 2104 cm^{-1} and 2032 cm^{-1} and a weak shoulder at 2060–2070 cm^{-1}. The following spectra (b–f) show that for CO exposures at increasing pressure the intensity of the original doublet decreases and three new bands evolve at 2189 cm^{-1}, 2159 cm^{-1} and 2086 cm^{-1}.

The bands at 2098 cm^{-1} and 2073 cm^{-1} are predominant in the spectrum of the specimen prepared by the procedure (A) and exposed to CO at higher pressure (8×10^{3} Pa, Fig. 4a). The influence of temperature is followed in the range 300–523 K. The initial bands are gradually replaced by a doublet at 2100 cm^{-1} and 2029 cm^{-1} (Fig. 4c,d) and restored during subsequent cooling in CO from 523 K to 300 K (Fig. 4f and g).

Fig. 5 demonstrates the changes of the spectra obtained by treatment B in the course of the temperature programmed CO desorption. The initial spectrum (Fig. 5a) is identical to the spectrum shown in Fig. 3f. The following spectra (b–g) demonstrate full reversibility of the spectral alternations resulting in the appearance of the spectrum 5g at 573 K which is completely identical to spectrum 3a. The bands at 2159 cm^{-1} and 2189 cm^{-1} disappear synchronously between 333–353 K, the band at 2086 cm^{-1} has vanished at 493 K and

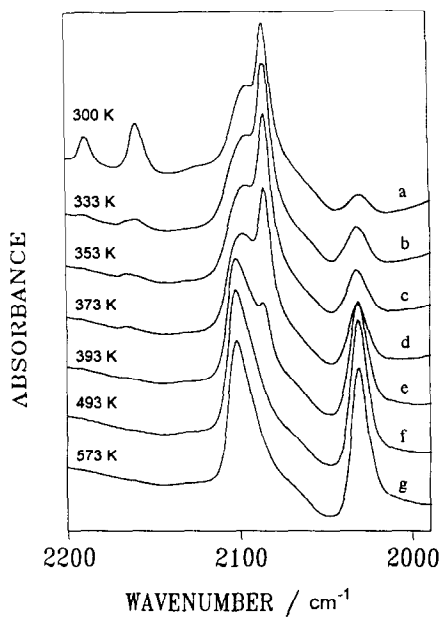

Fig. 5. Temperature programmed (5 K min^{-1}) desorption of CO adsorbed on the sample prepared by treatment B. Spectrum (a) is identical to spectrum (f) in Fig. 3.

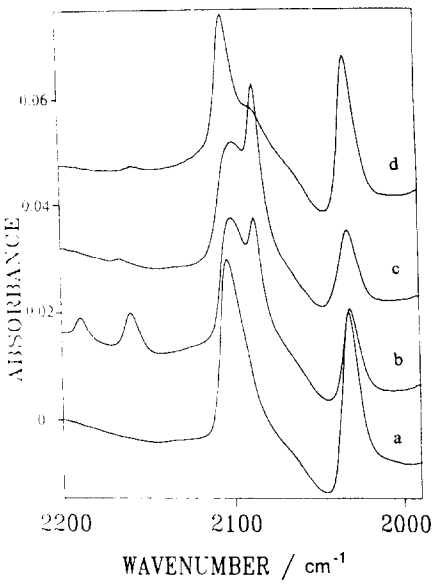

Fig. 6. IR spectra of Ir/H-ZSM-5 with preadsorbed CO: (a) CO adsorption at 1 Pa at 300 K followed by evacuation at 473 K, (b) CO adsorption at 10^4 Pa for 5 min at 300 K, (c) vacuum treatment at 373 K, (d) oxygen adsorption at 10^3 Pa at 373 K.

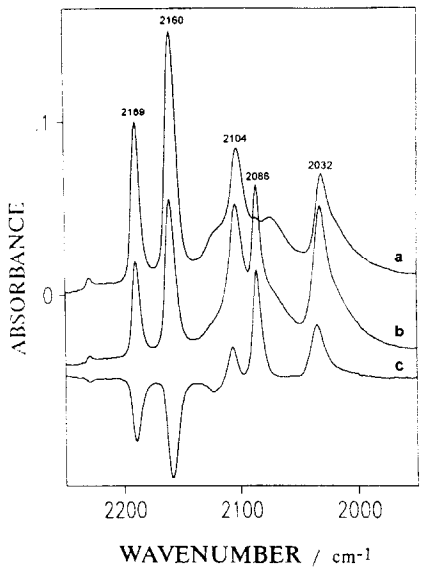

Fig. 7. IR spectra of Ir/H-ZSM-5, (a) after high-temperature treatment in CO (10^4 Pa at 523 K for 3 h) followed by evacuation for 1 min, (b) evacuation for 30 min, (c) difference spectrum of spectra (a) and (b).

only a doublet at 2104 cm^{-1} and 2032 cm^{-1} remains stable at 573 K.

Adsorption of CO (10^4 Pa, 5 min) at 300 K leads to the restoration of the spectrum previously shown in Fig. 5a (Fig. 6b). Subsequent temperature programmed desorption at 373 K removed the bands at 2189 and 2159 cm^{-1} (Fig. 6c) while additional treatment in oxygen at this temperature (10^3 Pa, 15 min) is necessary to remove the band at 2086 cm^{-1}. The doublet at 2104 cm^{-1} and 2032 cm^{-1} remained under these conditions unchanged (Fig. 6d).

Treatment C leads to the spectra shown in Fig. 7. After CO evacuation for 1 min the spectrum consists of four strong bands at 2189 cm^{-1}, 2159 cm^{-1}, 2104 cm^{-1} and 2032 cm^{-1} and of shoulders at ca. 2085 cm^{-1} and 2073 cm^{-1} (Fig. 7a). This spectrum is very similar to that depicted in Fig. 3d except the bands at 2189 cm^{-1} and 2159 cm^{-1} are more intensive. Prolonged evacuation at room temperature (Fig. 7b) leads to the decrease of the intensity of the two high-frequency bands and synchronous increase of three remainder bands which is most obvious from the difference spectrum (Fig. 7c).

4. Discussion

4.1. Assignment of FTIR CO bands

The variety of the bands observed under the influences of time, temperature and CO pressure demonstrates a rather complicated Ir carbonyl chemistry in zeolite ZSM-5. The band at 2062–2064 cm^{-1} observed at very low coverages of CO (Fig. 2b) can be ascribed to carbon monoxide linearly bonded to Ir^0 clusters whereas a broad band in the region of 1900–1910 cm^{-1} belongs to the bridged CO. CO adsorbed on the zeolite support also contributes to this band. This assignment is based on the numerous similar observations for Ir-loaded NaY, alumina and silica [5–9,11,20] where CO adsorption on Ir^0 clusters resulted in the band of linear CO at ca. 2035 cm^{-1} [9]. The observed shift of ca. 30 cm^{-1} for Ir/H-ZSM-5 might be related to a more electrophilic character of Ir^0 species in a highly acidic matrix [21] as well as to dipolar coupling in the adsorbed layer. The band of Ir^0–CO is very readily replaced either by two strong and sharp bands at 2104 cm^{-1} and 2032 cm^{-1} (Fig. 3a) or by three bands at 2098 cm^{-1}, 2073 cm^{-1} and 2032 cm^{-1} (Fig. 2d). The

Table 2
Identification of $Ir^{+}(CO)_2$ and $Ir^{3+}(CO)_2$ carbonyls by ligand exchange with isotopic labelling by ^{13}CO

Species	Wavenumber (cm^{-1})	
	Observed	Calculated
$Ir^{+}(CO)_2$	2104, 2032	2103, 2030
$Ir^{+}(CO)(^{13}CO)$	2087, 2000	2086, 2001
$Ir^{+}(^{13}CO)_2$	2053, 1985	2056, 1985
$Ir^{3+}(CO)_2$	2189, 2160	2193, 2160
$Ir^{3+}(CO)(^{13}CO)$	2182, 2126	2181, 2124
$Ir^{3+}(^{13}CO)_2$	2147, 2111	2144, 2122

doublet with two sharp bands separated by 70–80 cm^{-1} and located between 2000 cm^{-1} and 2100 cm^{-1} has been frequently observed in the literature [6,11–13,20] and was assigned to $Ir^{+}(CO)_2$ gem-dicarbonyl. Such assignment for the bands at 2104 cm^{-1} and 2032 cm^{-1} is confirmed by the experimental and calculated frequencies of ligand exchange obtained with a mixture of $^{13}CO^{12}CO$ (Table 2). The calculations were based on the energy factored force field [22] and carried out with the help of a program by Fuhrer et al. [23]. The parameters were calculated for a dicarbonyl with C_{2v} symmetry and for the wavenumbers 2104 cm^{-1} and 2032 cm^{-1}. Gelin et al. [9] assigned a doublet at 2086 cm^{-1} and 2003 cm^{-1} to $Ir^{+}(CO)_2$ in NaY. Later the same group [11] also observed a less intense doublet at 2102 cm^{-1} and 2030 cm^{-1} which is exactly the same as it was found for Ir/H-ZSM-5. The difference in the wavenumbers for similar species can be explained by their different geometry and stabilizing ligands. Most likely gem-dicarbonyl in H-ZSM-5 can be stabilized by zeolite oxygens.

The spectrum depicted in Fig. 2c appears to represent $Ir^{+}(CO)_2$ and another carbonyl species which is characterized by two principal bands at 2098 cm^{-1} and 2073 cm^{-1}. In this case the component at 2104 cm^{-1} is strongly overlapped with the more intense band at 2098 cm^{-1} and thus not visible. The band at 2032 cm^{-1} can also be attributed to both the remainder di-carbonyl and a new carbonyl species. The estimated intensity of the former peak should be at least three times lower, based on a constant ratio of the components in the doublet of gem-dicarbonyl. The bands at 2098 cm^{-1} and 2073 cm^{-1} are observed in CO atmosphere only and they disappear either during evacuation at room temperature or during CO treatment at higher temperature (473 K), pointing to a product of further Ir carbonylation. A reasonable candidate seems to be tetra-iridium cluster carbonyl, $Ir_4(CO)_{12}$, the formation of which in NaY was recently identified by FTIR [12–15]. $Ir_4(CO)_{12}$ sublimated onto IR cell window gives two strongest bands at 2056 and 2040 cm^{-1} which shift in NaY to 2070 cm^{-1} and 2032 cm^{-1} correspondingly (Table 3). Since the $Ir^{+}(CO)_2$ doublet in ZSM-5 is shifted by ca. 30 cm^{-1} as compared to that in NaY, it might be expected that a corresponding shift would occur for $Ir_4(CO)_{12}$ species. This assumption allows us to assign the bands at 2098 cm^{-1} and 2073 cm^{-1} as well as the band at 2032 cm^{-1} to tetra-Ir carbonyl in ZSM-5. The separation of 25 cm^{-1} and the relative intensities of the components are rather similar to those determined for individual $Ir_4(CO)_{12}$ (Table 3).

The absolute values of the frequencies depend on the geometry of the complex and are quite different for the individual compounds synthesized in the cages of NaY zeolite (Table 3). The assignment of the bands at 2100 cm^{-1} and 2087–2080 cm^{-1} to $Ir^{+}(CO)_3$ in NaY proposed in [24] looks less reasonable, especially if the chemistry of carbonylation–decarbonylation will be compared for ZSM-5 and NaY zeolites (see next sec-

Table 3
IR bands of Ir carbonyl species and their assignments

Species	Matrix	IR bands, cm^{-1}			Ref.
$Ir_4^0(CO)_{12}$	sublimed	2056	2040sh	2020	[12]
$[Ir_4(CO)_{11}Cl]^{1-}$	THF	2040	2005	1835	[12]
$Ir_4^0(CO)_{12}$	γ-Al_2O_3	2062	2040m	2024	[12]
$Ir_4^0(CO)_{12}$	NaY	2070	2060sh	2032	[13]
Ir_4^0–CO	NaY		2035		[13]
$Ir^{+}(CO)_2(acac)$	NaY	2070		2000	[13]
$Ir^{+}(CO)_2$	NaY	2086		2002	[9]
$Ir^{+}(CO)_2$	γ-Al_2O_3	2107		2137	[5]
$Ir_6^0(CO)_{16}$	NaY	2100	2064w	1730	[14]
$Ir^{+}(CO)_2$	H-ZSM-5	2104	2032		this work
$Ir_4^0(CO)_{12}$	H-ZSM-5	2098	2073	2032	this work
$Ir^{3+}(CO)_2$	H-ZSM-5	2189	2160		[9,11]

tion). The absence of any reliable assignment of $Ir^+(CO)_3$ should be also noted. Gelin et al. [11] originally ascribed similar bands to tricarbonyl, however, later the same doublet was assigned to dicarbonyl species of iridium [9].

Three different bands at 2160 cm^{-1}, 2189 cm^{-1} and 2085–2086 cm^{-1} have been observed for Ir/H-ZSM-5 pretreated with CO at rather high pressures (10^2–10^4 Pa) (Fig. 3, b–f and Fig. 5 a and b). These bands normally co-exist with the doublet of $Ir^+(CO)_2$. The high frequency peaks at 2189 cm^{-1} and 2159 cm^{-1} behave as a doublet synchronously disappearing either at prolonged evacuation at room temperature or during heating at 333–353 K. The assignment to $Ir^{3+}(CO)_2$ is confirmed by isotopic labeling (Table 2). Previously single bands located either at 2185 cm^{-1} or at 2100 cm^{-1} were tentatively assigned to $Ir^{3+}(CO)_2$ species [9,11]. An intense band at 2086 cm^{-1} appeared simultaneously with the $Ir^{3+}(CO)_2$ doublet. The general features of this band are:

1. it is observed after pretreatment in CO at rather high pressures (10^3–10^4 Pa) either at room temperature (Fig. 3b–e) or at 523 K (Fig. 7a and b);
2. it is observable only after sample evacuation;
3. it is always associated with the bands belonging to $Ir^{3+}(CO)_2$ and $Ir^+(CO)_2$;
4. the difference spectra (Fig. 7c) indicate that the intensity of this band and the doublet of $Ir^+(CO)_2$ increase synchronously with a decrease of the bands belonging to $Ir^{3+}(CO)_2$;
5. the band is stable in vacuum up to 393 K (Fig. 5e) but almost completely disappeared after treatment with oxygen at the same temperature (cf. Fig. 6c and 6d).

The characteristics of the band at 2086 cm^{-1} allow the assignment to CO linearly bonded to highly dispersed $Ir^{\delta+}$ clusters. The additional upward shift by more than 20 cm^{-1} with respect to the band of CO bonded to initially formed Ir^0 clusters (Fig. 2b) could be explained by a higher electron deficiency of newly formed $Ir^{\delta+}$ species. Although higher CO coverage could be expected for static conditions of CO adsorption, the absence of any noticeable shift of the band at 2086 cm^{-1} upon the thermodesorption excludes another possible explanation, i.e. an upward shift based on a dipole–dipole interaction. The sensitivity to oxygen supports the present identification of the band as Ir^0–CO. Similarly, Gelin et al. [9] ascribed the band at 2060–2070 cm^{-1} which co-existed with $Ir^+(CO)_2$ species in NaY to CO linearly attached to Ir^0. As in our case, the band vanished after oxygen treatment at 373 K. It was shown also by Solymosi et al. for Ir/Al_2O_3 [5] and for Rh/Al_2O_3 [25], that the formation of linearly bonded CO can occur by reductive agglomeration of gem-dicarbonyl species followed by the restoration of Me^0 clusters.

4.2. Chemistry of Ir carbonyls in the ZSM-5 structure

XPS yields the information on the oxidation states and effective charge of the Ir adsorption sites. Most of the Ir cations in the as-prepared sample have a BE value similar to the precursor complex $[Ir(NH_3)_5(H_2O)]Cl_3$. Formally, the binding energy of Ir $4f_{7/2}$ (64.0 eV) found for ca. 25% of the iridium complex ions in the as-prepared sample, could be assigned to the Ir(IV) state observed for IrO_2 species on supports [26]. Our previous work [21] revealed this state after high-temperature calcination of the impregnated Ir/H-ZSM-5. However, the sample studied in this work was not subject to any treatment in air at elevated temperatures (it was dried at ambient temperature). Therefore the formation of Ir(IV) is very unlikely. No time-dependent changes of the spectra were observed during the measurements and therefore a change of the Ir oxidation state caused by X-ray radiation can be confidently ruled out. The increase of the BE for cations with the same formal oxidation state placed in zeolites is not surprising and was frequently observed, for example, for Rh(III), Ru(III), Pd(II) (see references in the monograph [17] and other works [27–29] and has been explained by the effect of the strong electrostatic field of the zeolite framework as well as by the increase of effective positive charge on

the metal cations. It is likely that Ir(III) cations under evacuation at room temperature became partially coordinated with zeolitic framework oxygen (water and/or ammonia ligands can be displaced) which results in the observed increase of the binding energy for the minority of Ir species.

For reduced Ir/H-ZSM-5, two major Ir sites can be identified. One, characterized by a BE of Ir $4f_{7/2}$ equal to 63.4 eV, definitely belongs to Ir^{3+} cations. A similar value, 62.9 eV, was determined for Ir^{3+} in NaY [11]. The difference of 0.5 eV could be attributed to the slightly different environment of Ir cations. The high N/Si ratio observed for the sample prereduced at 423 K indicates that Ir^{3+} cations remained partially coordinated by NH_3 ligands.

Another Ir 4f doublet (Fig. 1b) has a maximum of Ir $4f_{7/2}$ at 62.0 eV, which is by 1.4 eV higher than the BE for bulk iridium metal. This spectrum could be assigned to very dispersed Ir^0 clusters exhibiting strong electron deficiency in the highly acidic zeolite matrix. A similar value of BE shifts has been determined for small clusters of Pt in H-ZSM-5 [21], Pd in H-ZSM-5 [29] and HY [30]. The relaxation term would also contribute to these shifts. As was shown in determining the Auger parameter, however, it will not cover the large BE shift observed for Pd in HY [30] and for Ir in H-ZSM-5 [31]. No particles were detected by TEM in the Ir/H-ZSM-5 reduced at 423 K which could mean that their diameter is less than 1 nm. However, Ir/H-ZSM-5 prepared by impregnation and reduced at 623 K yields particles in the range between 1 and 3 nm exhibiting a lower BE of Ir $4f_{7/2}$ equal to 61.1 eV [31]. The higher reduction temperature and the appearance of $Ir^{\delta+}$ clusters indicate, that the reduction of Ir^{3+} cations is impeded in H-ZSM-5 as compared to Ir/NaY, where lower reduction temperatures and only Ir^0 particles have been observed [9].

The formation of Ir^0 clusters in reduced Ir/H-ZSM-5 is confirmed by the presence of a CO band at 2062 cm^{-1} which belongs to CO linearly bonded to Ir metallic particles (Fig. 2b). Similar frequencies at rather similar coverages have been observed for Ir/NaY [9] and Ir/H-ZSM-5 containing well-defined metallic particles [28]. If it is assumed that the shift caused by dipolar coupling for smaller particles will be smaller than for larger particles, which is not unreasonable [32,33], higher singleton frequencies of linear CO can be expected for the Ir/H-ZSM-5 compared to other supports [6,9]. At a first glance, this contradicts with the assignment of the large XPS shift to very small Ir clusters. However, this discrepancy is apparent since the CO stretching frequency is the function of both particle size and metal–support interaction. For well-defined platinum clusters of similar size (10–15 atoms) very different frequencies have been found in highly acidic H-ZSM-5 (2080–2090 cm^{-1}) [18] and basic KL zeolite supports (2000–1925 cm^{-1}) [33,34] which clearly manifests a large contribution of metal–support interaction. The same is the case with Ir-loaded zeolites. Therefore the formal coincidence of the frequencies observed with larger metallic particles on NaY and smaller metallic particles (clusters) in H-ZSM-5 can be plausibly explained by a larger electron deficiency of the metal clusters in H-ZSM-5 which results in the additional upward shift in CO FTIR spectra.

Other convincing proof of the metal clusters is the very rapid formation of $Ir^+(CO)_2$ even with residual CO (Fig. 3a) which shows that the Ir^0 clusters are not stable and undergo oxidation to the Ir^+ state. It is believed that Ir^0 can be reoxidised by protons belonging to the bridged OH groups similarly to Rh^0 clusters in HNaY zeolites [35,36]:

$$Ir^0 + H^+ + 2CO \rightarrow Ir^+(CO)_2 + \tfrac{1}{2}H_2 \qquad (1)$$

Actually, a first stage of this reaction is the formation of $Ir^{(\delta+)}H^{(\delta-)}$ adducts well-defined for Pd, Rh and Pt [37] in Y zeolites, which was additionally confirmed by synchronous upward shifts both in XPS and FTIR spectra. As was mentioned above, gem-dicarbonyl is most likely coordinated with water or OH group. Similar chemistry of particle disruption with CO was found for larger Rh particles [28,35]. However, rhodium is known to be less noble and more oxophilic than iridium. Indeed, iridium particles with average size of 1.8

nm mostly located on the external surface of the H-ZSM-5 have nearly the same wavenumbers of linearly adsorbed CO, however they could not be converted to $Ir^+(CO)_2$ under similar conditions [32].

Further carbonylation of a $Ir^+(CO)_2$ complex via water–gas shift reaction with formation of tetra-Ir cluster carbonyl is proposed

$$4Ir^+(CO)_2 + 2H_2O + 6CO \rightarrow Ir_4(CO)_{12} + 4H^+ + 2CO_2 \quad (2)$$

The spectra indicate that a balance between gem-dicarbonyl and cluster carbonyl always exist. The product of reductive carbonylation, i.e. $Ir_4(CO)_{12}$, is unstable and it readily decarbonylates into $Ir^+(CO)_2$ under evacuation at room temperature or under heating in CO at elevated temperatures.

Taking into consideration the geometry and size of ZSM-5 channels one could speculate on the possible location of tetra-Ir carbonyl and on a mechanism of carbonylation–decarbonylation. The product of $Ir^+(CO)_2$ carbonylation is most likely a tetra-carbonyl species. It was characterized by three bands: 2098 cm^{-1}, 2073 cm^{-1} and 2033 cm^{-1} (Table 3), two of them are very similar to those observed in NaY by Kawi et al. [13]. In their case $Ir_4(CO)_{12}$ was additionally characterized by EXAFS. It is not unlikely that $Ir_4(CO)_{12}$ has a distorted geometry in ZSM-5 and therefore shows additional peaks, i.e. at 2100 cm^{-1}. According to [13] the size of the $Ir_4(CO)_{12}$ molecule is ca. 9 Å. It consists of a tetrahedral frame with each Ir atom bonded to 3 neighbors at a distance of 2.69 Å and to three terminal carbonyl ligands having distances Ir–C, 1.87 A and Ir–O, 3.01 Å which gives the largest linear size of about 7.6 Å. From these very simple geometric considerations it is probable that $Ir_4(CO)_{12}$ can be accommodated in the ZSM-5 channel intersections with a diameter of 9 Å, provided some of the CO ligands could be expanded into the channels. Molecular dynamic modeling is necessary to prove this. Similar to $Rh_4(CO)_{12}$ in Y zeolite [37] the iridium cluster carbonyl could also be located in the larger internal voids of ZSM-5 like in the case of metallic platinum particles [38].

On the other hand, location of $Ir_4(CO)_{12}$ on the external surface, as it was observed for silica-supported iridium species [39] is less probable and contradicts with the reversibility of the carbonylation–decarbonylation process observed in H-ZSM-5.

Kawi et al. [12–15] by using a combination of FTIR and EXAFS found that $Ir_4(CO)_{12}$ was decarbonylated into naked Ir clusters which retain the tetrahedral frame in the cages of NaY. In their case decarbonylation was observed in the course of heating $Ir_4(CO)_{12}$ either in hydrogen or in an inert atmosphere. It is also possible that the formation of an Ir_4 cluster is a first step of the decarbonylation of tetra-Ir carbonyl in ZSM-5:

$$Ir_4(CO)_{12} \rightarrow Ir_4 + 12CO \quad (3)$$

The intermediate Ir cluster could then interact with protons and traces of CO according to the reaction (1) to form the most stable compound, i.e. the gem-dicarbonyl. In the slightly basic NaY such reaction is hindered. Carbonylation chemistry in ZSM-5 seems to be restricted to tetra nuclear cluster while on other supports $Ir_4(CO)_{12}$ serves normally as an intermediate to produce $Ir_6(CO)_{16}$. The latter was observed in NaY by Bergeret et al. [7] and recently by Kawi et al. [12–15]. The formation of the hexacarbonyl species, however, is not favored in ZSM-5 owing to the limitations of the intracrystalline space.

Thus, the strong proof in favour of $Ir_4(CO)_{12}$ formation in ZSM-5 is the similarity in the behaviour of iridium clusters and carbonyls in ZSM-5 and well-defined carbonyls of $Ir^+(CO)_2$ and $Ir_4(CO)_{12}$ in NaY, Al_2O_3, MgO and SiO_2 [12–15,40]:

1. In both zeolites (ZSM-5 and NaY) $Ir_4(CO)_{12}$ forms on the reaction with CO and water and always is in an equilibrium with $Ir^+(CO)_2$. This reaction is fully reversible at room temperature.
2. $Ir_4(CO)_{12}$ is decarbonylated under vacuum (ZSM-5) or under He or H_2 (NaY) with formation of Ir_4 cluster. In our case the Ir cluster

band is obscured by very strong bands of the $Ir^+(CO)_2$ but still can be seen as a weak shoulder at ca. 2070 cm^{-1} (Fig. 2e).

3. The difference between these species on two supports is lower stability of $Ir_4(CO)_{12}$ in ZSM-5 explained above by very tight space in Pentasil.

Another interesting feature of CO interaction with Ir/ZSM-5 is the formation of $Ir^{3+}(CO)_2$. This carbonyl was observable after CO pretreatments at rather high pressure particularly at elevated temperature (523 K). In the latter case the bands of $Ir^{3+}(CO)_2$ were most intense. This was unexpected since CO treatment should result in a partial reduction of Ir^{3+} cations via the water–gas shift reaction. The high intensity of $Ir^{3+}(CO)_2$ might be explained by the fact that Ir^{3+} cations, still present in the prereduced sample, are coordinated to NH_3 ligands and initially have low ability to adsorb CO. The intense N–H stretchings observed in FTIR spectra support this assumption. However, at higher pressures CO is able to displace NH_3 ligands from the Ir coordination sphere. $Ir^{3+}(CO)_2$ can be readily decomposed by evacuation or under mild heating. The changes of the relative intensities for $Ir^{3+}(CO)_2$, $Ir^+(CO)_2$ and species ascribed to Ir^0–CO during evacuation or thermodesorption indicate that decomposition of $Ir^{3+}(CO)_2$ is accompanied by stepwise reduction, i.e.

$$Ir^{3+} \rightarrow Ir^+ \rightarrow Ir^0 \qquad (4)$$

Although the mechanism of this process is not clear one could assume that desorbed CO and water reduce Ir^{3+} and Ir^+ cations via the water–gas shift reaction, and that a part of the CO is readsorbed on Ir^+ and Ir^0 species to produce more stable $Ir^+(CO)_2$ and Ir^0–CO complexes.

The similarity to rhodium chemistry should be pointed out, although for rhodium at room temperature all transformations shown by sequence (4) will be shifted to the left. Rhodium clusters can be very easily disrupted into $Rh^+(CO)_2$ or even into $Rh^{3+}(CO)_2$ species at room temperature, however, their reductive agglomeration and the formation of Rh metal particles occurs at elevated temperatures [25,28,35,40].

5. Conclusions

Various Ir carbonyl species are formed during CO adsorption on Ir^0 clusters and Ir^{3+} cations located inside the channels of H-ZSM-5. In the carbonylation of zerovalent Ir the reoxidation of small Ir^0 clusters by protons is the very first step of these transformations. In CO atmosphere, gem-dicarbonyl $Ir^+(CO)_2$ located in the channel intersections is assembled into a larger cluster most likely tetra-Ir carbonyl which is unstable and decomposes into an initial precursor compound at higher temperatures or lower CO pressures. This carbonylation–decarbonylation cycle is reversible in the range of CO pressures between 1 Pa and 10^4 Pa and temperatures between 300 K and 523 K.

Ir^{3+} cations can be also carbonylated to form $Ir^{3+}(CO)_2$. The decomposition of this complex is accompanied by stepwise reduction of Ir^{3+} to Ir^+ and to Ir^0 due to water–gas shift reaction manifested by additional formation of $Ir^+(CO)_2$ and Ir^0–CO.

Acknowledgements

Support by the Deutsche Forschungsgemeinschaft (AZ 438 113-139) is gratefully acknowledged. TVV and ESS want to acknowledge financial support by the Russian Foundation of Fundamental Researches (93-03-5549) and the International Science Foundation (MM1 000).

References

[1] L. Rao, A. Fukuoka and M. Ichikawa, Shokubai, 31 (1989) 64.
[2] R. Myrdal and S. Kolboe, Stud. Surf. Sci. Catal., 46 (1989) 327.
[3] F. Lefebvre, P. Gelin, B. Elleuch, Y. Diab and Y. Ben Taarit, Stud. Surf. Sci. Catal., 18 (1984) 257.

[4] R.W. Rice and K. Lu, J. Catal., 77 (1982) 104.
[5] F. Solymosi, E. Novak and A. Molnar, J. Phys. Chem., 94 (1990) 7250.
[6] F.J.C.M. Toolenaar, A.G.T.M. Bastein and V. Ponec, J. Catal., 82 (1983) 35.
[7] G. Bergeret, F. Lefebvre and P. Gallezot, in Y. Murakai, A. Iijima and J.W. Ward (Eds.), New Developments in Zeolite Science Technology, Proceedings 7th International Zeolite Conference, Tokyo, 1986, Kodansha, Tokyo, 1986, p. 401.
[8] H. Bischoff, N.I. Jaeger and G. Schulz-Ekloff, Catal. Today, 8 (1991) 501.
[9] P. Gelin, A. Auroux, Y. Ben Taarit and P.C. Gravelle, Appl. Catal., 46 (1989) 227.
[10] O.B. Yang, S.I. Woo and R. Ryoo, J. Catal., 137 (1992) 557.
[11] P. Gelin, G. Coudurier, Y. Ben Taarit and C. Naccache, J. Catal., 70 (1981) 32.
[12] S. Kawi, J.-R. Chang and B.C. Gates, J. Phys. Chem., 97 (1993) 5375.
[13] S. Kawi, J.-R. Chang and B.C. Gates, J. Phys. Chem., 97 (1993) 10599.
[14] S. Kawi and B.C. Gates, J. Chem. Soc., Chem. Commun., (1991) 994.
[15] S. Kawi, J.-R. Chang and B.C. Gates, J. Am. Chem. Soc., 115 (1993) 4830.
[16] W. Palmaer, Z. Anorg. Allg. Chem., 10 (1895) 320.
[17] Kh.M. Minachev and E.S. Shpiro, The Catalyst Surface: Physical Methods of Studying, CRC Press, Boca Raton, FL, 1990.
[18] O.P. Tkachenko, E.S. Shpiro, N.I. Jaeger, R. Lamber and G. Schulz-Ekloff, Catal. Lett., 23 (1994) 251.
[19] A. Tonscheidt, P.L. Ryder, N.I. Jaeger and G. Schulz-Ekloff, Surf. Sci., 288 (1993) 51.
[20] O.I. Smith and W.C. Solomon, Ind. Eng. Chem. Fund., 21 (1982) 374.
[21] T.V. Voskobojnikov and E.S. Shpiro, Kinet. Katal., 34 (1993) 321.
[22] P.S. Braterman, Metal Carbonyl Spectra, Academic Press, London, 1975, p. 36ff.
[23] H. Fuhrer, V.B. Kartha, K.G. Kidd, P.J., Krueger and H.H. Matsch, N.R.C.C. Bulletin, 166 (1986) 347.
[24] F. Lefebvre, A. Auroux and Y. Ben Taarit., Stud. Surf. Sci. Catal., 24 (1984) 411.
[25] F. Solymosi and M. Pasztor, J. Phys. Chem., 89 (1985) 4789.
[26] J. Burkhardt and L.D. Schmidt, J. Catal., 116 (1989) 240.
[27] E.S. Shpiro, G.J. Tuleuova, V.I. Zaikovsky, O.P. Tkachenko and Kh.M. Minachev, Kinet. Katal., 30 (1989) 939.
[28] T.T.T. Wong, A. Yu. Stakheev and W.M.H. Sachtler, J. Phys. Chem., 96 (1992) 7733.
[29] Kh.M. Minachev, G.V. Baeva, E.S. Shpiro and A.B. Phasman, Kinet. Katal., 26 (1985) 1265.
[30] A.Yu. Stakheev and W.M.H. Sachtler, J. Chem. Soc., Faraday Trans., 87 (1991) 3709.
[31] T.V. Voskobojnikov and E.S. Shpiro, unpublished results.
[32] A. de Mallmann and D. Barthomeuf, Stud. Surf. Sci. Catal., 46 (1989) 429.
[33] M.J. Kappers and J.H. van der Maas, Catal. Lett., 10 (1991) 365.
[34] A.Yu. Stakheev, E.S. Shpiro, N.I. Jaeger and G. Schulz-Ekloff, Catal. Lett., 32 (1995) 147.
[35] D.C. Tomczak, V.L. Zholobenko, H. Trevino, G.-D. Lei and W.M.H. Sachtler, Stud. Surf. Sci. Catal., 84 (1994) 893.
[36] G. Bergeret, P. Gallezot, P. Gelin, Y. Ben Taarit, F. Lefebvre, C. Naccache and R.D. Shannon., J. Catal., 104 (1987) 279.
[37] W.M.H. Sachtler, Catal. Today, 15 (1992) 419.
[38] E.S. Shpiro, R. Joyner, Kh.M. Minachev and P.D.A. Pudney, J. Catal., 127 (1991) 366.
[39] R. Psaro, D. Roberto, R. Ugo, C. Dossi and A. Fusi, J. Mol. Catal., 74 (1992) 391.
[40] P. Johnston, R.W. Joyner, P.D.A. Pudney, E.S. Shpiro and B.P. Williams, Faraday Discuss. Chem. Soc., 89 (1990) 91.